AMV Height assignment methods with Meteosat-8

Régis Borde

EUMETSAT, Am Kavalleriesand 31, 64295 Darmstadt, Germany

Abstract

Several sources of error can be introduced at the height assignment (HA) step in the Atmospheric Motion Vector (AMV) extraction scheme, including the sensitivity of the HA methods themselves. But one of the main difficulties is due to the pixel selection process, which links the height calculation to the feature that drives the tracking in the tracer box. The most common method sorts the coldest pixels to calculate the height. Then NOAA/NESDIS uses a fix threshold of 25% coldest pixels for GOES instrument, whereas EUMETSAT uses the coldest cluster inside the target area for Meteosat 8. In the EUMETSAT AMV HA scheme the separation of the clusters is based on two output parameters of the Cloud Analysis (CLA) step: the cloud phase and the cloud top height (CTH). Unfortunately, the use of these criteria may induce a large error into the calculation of the pressure, especially in tricky multilevel cloudy situations, or/and when several types of clouds are present together in the target box. This study presents an example of such error, and shows the benefits of using several percentages of the cloudy pixels present in the target area instead of the current clustering scheme used at EUMETSAT. The consistency of all the methods implemented to calculate the AMV height with Meteosat 8 is improving with the new approach, together with the estimation of the error associated with the pressure and the comparison against forecast data.

CLUSTERING PROBLEM

The aim of the clustering process is to sort the pixels inside the target area as function of physical criteria, in order to identify coherent features that are then called ‘clusters’. The pressure and EBBT of all identified clusters are calculated in the HA process. The EUMETSAT operational clustering is currently done using two parameters from the CLA output file: the Cloud Top Height (CTH) and the cloud phase: Water, Ice, and Mixte. More information about the CLA product can be found in the EUMETSAT Technical Memoranda: MSG - Cloud Processing, (TM-04). As the troposphere is divided in 5 bands of 200 hPa (100-300, 300-500, 500,700, 700-900 and >900 hPa), the cloudy pixels inside the target area can be sorted in 15 possible clusters (5 possible CTH bands x 3 possible cloud phases). More detailed information about this clustering process can be found in the EUMETSAT MSG Algorithm Specification Document (EUM.MSG.SPE.022).
The figure 1 shows a detailed example of an AMV target area extracted with the prototype code close to a big convective cell. The small square inside the radiance images (Vis008, IR108, WV062 and WV073) represents the 24x24 target area. Detailed information of the scene identification, the cloud phase, the cloud type and the cloud top height parameters of this target box are presented on the right side of the figure 1. The CTH is plotted on that figure as function of the 5 bands used to sort the pixels in clusters. Each colour corresponds to a cluster. The red cluster, which corresponds to the layer 100-300 hPa, is divided in two separate groups of pixels inside the target area. The first one, at the bottom right of the target box, corresponds to the big high convective cell clearly visible in the radiance images. This group is identified as an opaque high level cloud in ice phase. The second group of red pixels (middle top of the target box) is identified as a high level semi-transparent cloud, in ice phase as well. The correction of semi-transparency for this group of pixels has been done already during the cloud analysis step, which ended to a cloud top height between 100 and 300 hPa.

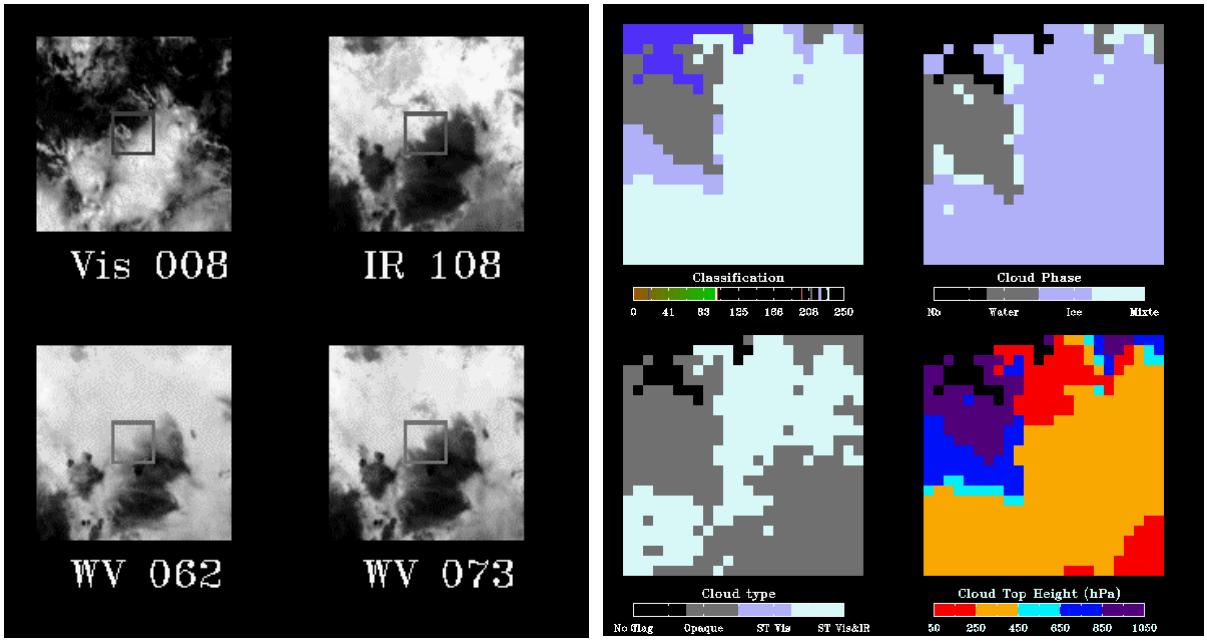

Figure 1 : Example of AMV vector detected over a big convective cell. Detailed information on the clustering and cloud analysis for the target area are shown on the right side.

Figure 2 shows the consequences of this clustering process on the AMV pressure calculated for this target area using STC method (Schmetz et al, 1993, Niemann et al., 1993) and EBBT method. On the WV/IR graph presented on the left side, the two groups of red pixels located inside the target area can be easily identified. The high level opaque group of red pixels corresponds to the cold radiances located on the Radiative Transfer Model (RTM) curve (solid line). The warmer radiances of the second group of red pixels present the linear dependence characteristic of the semi transparent clouds. The STC pressure is calculated from the slope between the representative clear sky radiance (in green on the graph) and the representative cloudy radiance of the cluster. As the red cluster is constituted by the cold radiance of the high opaque pixels and the warm radiance of the semi transparent pixels both together, the representative cloudy radiance of the red cluster is then located somewhere between the two groups of pixels, but it is in fact representative of no-one of them. Of course, this can lead large error in the calculation of STC pressure.

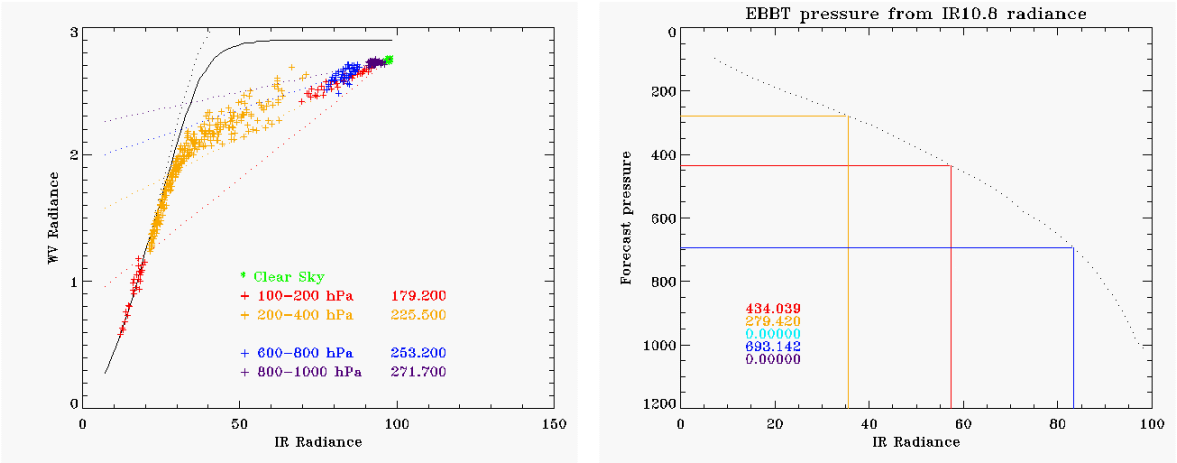

Figure 2: Impact of the current clustering on the STC (left) and EBBT (right) methods. The red cluster is clearly constituted by two groups of pixels that have very different physical properties.

The impact is again worst for the calculation of the EBBT pressure. This one derived directly from the IR108 radiances of the cluster interpolating the forecast profile. Mixing cold radiances of the high

opaque group of pixels and warm radiances of the semi transparent group of pixels both together ends to a final pressure located at midlevel in the troposphere, close to 430 hPa. Considering the two groups separately, the EBBT pressure is close to 180 hPa for the high opaque group of pixels (representative IR108 lower than 20) and 700 hPa for the semi transparent group of pixels (representative IR108 radiance nearly 80). The current situation, for which semi transparent clouds and high opaque clouds are present both together in the target box and classified into the same cluster may occur frequently, especially in tropical areas.

NEW CLUSTERING APPROACH

Method

The main problem is to clearly establish a link between the pixels that drive the tracking and the pixels selected to calculate the height of the AMV. According to the tracking method used at EUMETSAT (Dew and Holmlund, 2002), mainly based on the selection of the maximum contrast into the target box, the brightest pixels are dominating the tracking step in the VIS channel, when the coldest pixels dominate it in the IR channels. The main logical and common way to stick the HA calculation to the tracking feature is to select the pixels directly from image radiances, keeping brightest cloudy radiance for VIS channel, and darkest cloudy radiances for IR channel. The NOAA/NESDIS already uses a fix percentage of 25% coldest cloudy pixels using the CO2 slicing method with GOES instrument. A still open and difficult question is how many pixels are really dominating the tracking step and should then be used for the calculations. To leave up this problem, several percentages of coldest cloudy pixels (10%, 15%, 20% and 25 %) have been considered. The Figure 3 shows the result of the new clustering approach applied to the case described above, using the radiance of the IR108 channel. Red pixels correspond to the 10% coldest cloudy pixels, red+orange to the 15% …etc. Only the high opaque cloud located at the bottom right of the picture is then considered for the HA calculation.

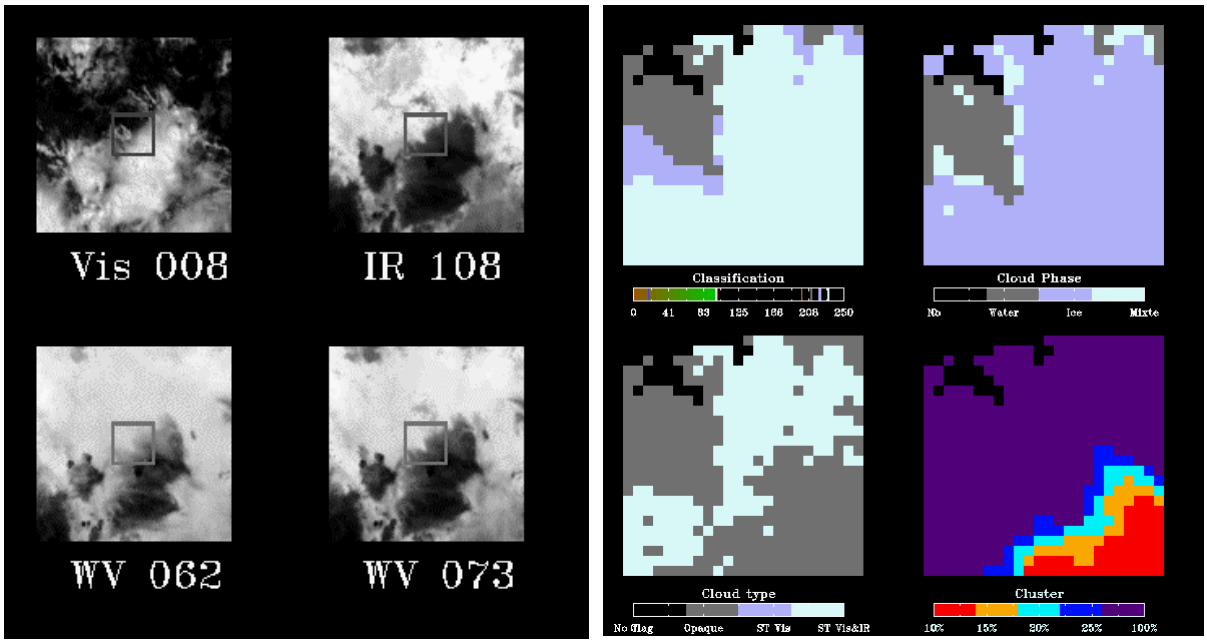

Figure 3: Result of the new clustering approach applied to the case described above.

Performance of the methods with new clustering approach

Figure 4 illustrates the performances of the STC method (left) and the EBBT method (right), using the new approach for the case study described above. This figure 4 should be compared to the figure 2 that illustrates the same plots for the current clustering. The new clustering scheme gives a coldest STC pressure 10 hPa higher in the atmosphere. Even if the red pixels are a bit scattered along the opaque RTM curve, the representative cloudy radiance of the 10% cloudy pixels is more representative of the red group than previously. The impact of the percentage can also be examined

on this figure. The pressure calculated by STC method is increasing from 170 hPa using the 10% cloudy pixels to 197 hPa using the 25 % cloudy pixels. That means the STC method is very sensitive, and a small variation of the pixel radiances can induce a big difference in pressure. That also makes an accurate estimation of the height very difficult.
Right graph of the figure 4 illustrates the impact on the EBBT pressure. This one is very impressive with more than 250 hPa difference between the pressure of the red cluster using the current clustering scheme, 434 hPa and the pressure of the 10% coldest cloudy pixels, 180 hPa. The EBBT pressure also varies very quickly increasing the percentage of coldest pixels used for the calculation. The EBBT pressure for the 10% coldest cloudy pixels is around 180 hPa as it increases to 203 hPa for the 25% percentage.
The pressure difference between the two clustering schemes using CO2 slicing method (Smith and Platt, 1979, Menzel, et al, 1983, Merill et al., 1991) is nearly 20 hPa for this case study, 162 hPa for the current clustering scheme, and 180 hPa for the 10 % new approach (graphs not shown). Considering the results for several percentages of coldest cloudy pixels, the CO2 slicing method appears very sensitive as well. The estimated pressure varies more than 20 hPa considering the 10% and 25 % coldest radiances.
The pressures calculated using the new clustering approach from CO2 slicing method and EBBT method are in a very good agreement. This is a good signal about the consistency of the result, because the 10% coldest pixels considered in that case study are really representative of a high opaque cloud. These two methods should then give a very similar result. Also the STC pressure is in good agreement with CO2 slicing and EBBT pressures within a range of 10 hPa.

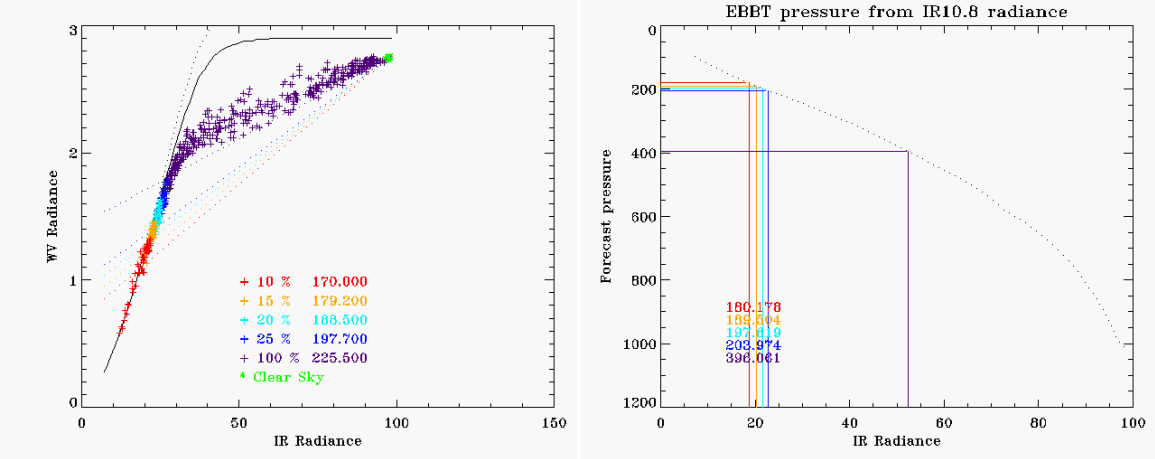

Figure 4: STC and EBBT methods performances using the new clustering scheme.

Consistency of the HA methods.

The STC and CO2 slicing methods aim both together at correcting the calculation of the cloud top height from the effect of cloud semi transparency. Consequently, the cloud top pressures calculated on the same data set, using these two methods, should theoretically be in a quite good agreement. Unfortunately, previous studies using Meteosat 8 data (Borde and Arriaga 2004, De Smet, 2004) and GOES data (Schreiner and Menzel, 2002, Schreiner et al., 2004) showed important discrepancies between the STC and CO2 slicing results, and the general agreement of these methods was not as good as expected. The results calculated by two different versions of the same method (STC6.2 and STC7.3 for example) had a general poor agreement between each other as well. A bias around 30 hPa has been noted between the CO2 slicing methods using the IR108 and IR120 Meteosat 8 channels respectively.
Comparing the results of STC and CO2 slicing methods provides information about the good performances of the methods themselves and about the consistency of the results as well. The Figure 5a presents such a comparison between STC and CO2 slicing pressures, using current clustering scheme (left side) and new clustering scheme for the 10% percentage of coldest cloudy pixels (right side). The dataset considered on these plots corresponds to 26600 AMVs extracted over the full disk from a triplet of Meteosat 8 images (29 March 2004 at 12:30 UTC). The two first plots (top) present the comparison of STC method using the WV073 versus the CO2 slicing method using the IR120, as the

two last plots show the results of the STC method using the WV062. The biases and correlation coefficients correspond to statistical information calculated considering only the green dots. These ones correspond to cases for which the CO2 slicing method is operationally used, which means that the temperature of the cluster is colder than 253 K.

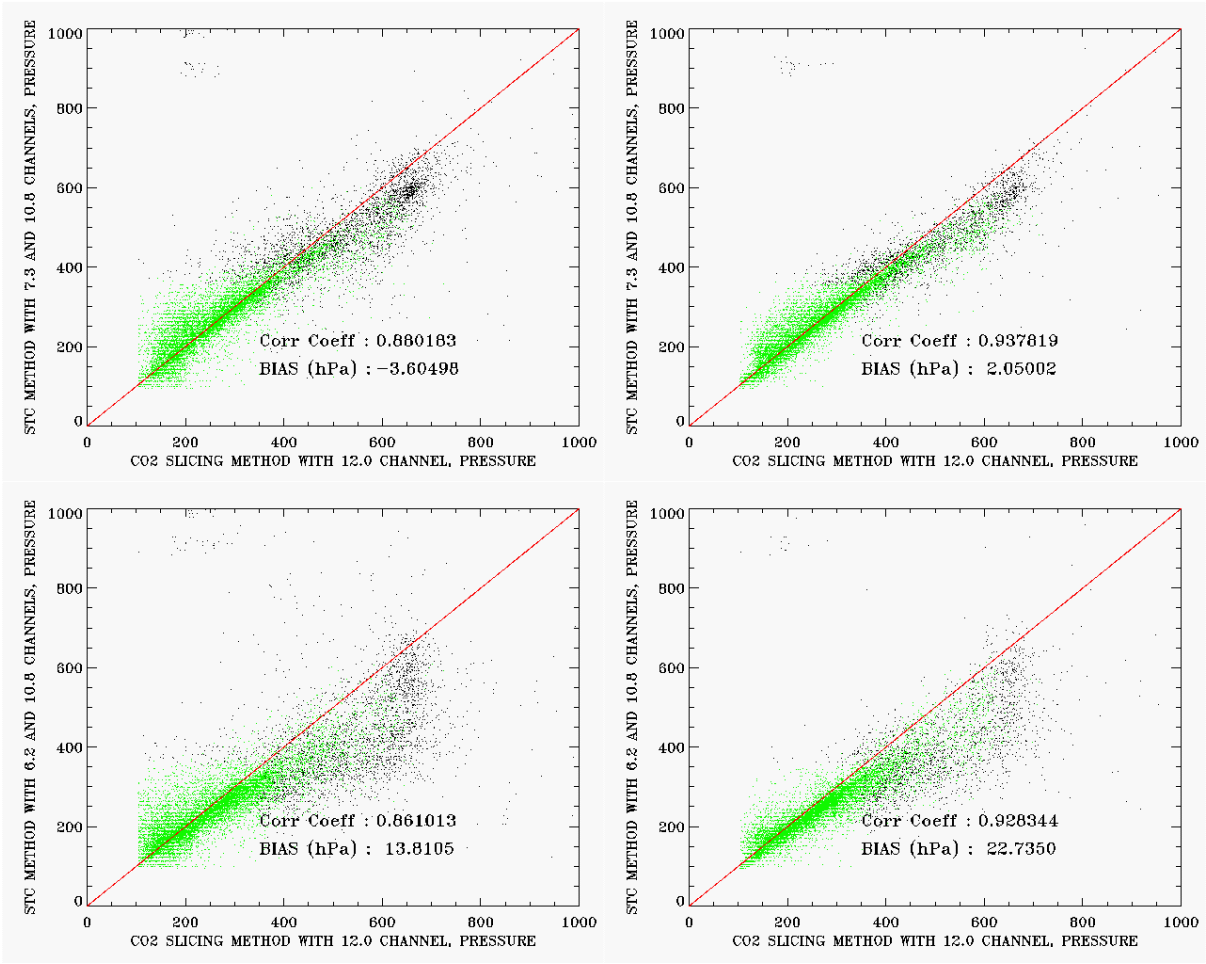

Figure 5a: Consistency of STC and CO2 slicing results. Current clustering scheme comparison is plotted on the left side and the new clustering approach comparison on the right side.

The new clustering approach clearly improves the agreement of STC and CO2 slicing methods between each other. The correlation coefficients are increasing from 0.88 (current clustering) to 0.94 (new clustering) for the STC version using the WV073, and from 0.86 (current clustering) to 0.93 (new clustering) for the STC version using the WV062. For the STC WV073 version, the bias is also very small, close to 2 hPa. The agreement using the WV062 is a bit worse than the one using the WV073, but the improvement of the new clustering scheme on the correlation coefficient is still very clear.
Figure 5b presents the consistency of two different versions of the same method between each other. Upper plots illustrate the agreement between CO2 slicing method using the channels IR108 and IR120, whereas the lower plots compare the results of the two STC versions, using the channels WV062 and WV073. The new clustering approach also increases the agreements between the various versions of the same method. The correlation coefficient for the two configurations of the CO2 slicing method is then very close to 1, and the bias is divided by a factor 2 comparing to the bias obtained using the current clustering. The correlation coefficient of the two STC versions increases from 0.86 to 0.93, and the bias remains unchanged, close to 25 hPa. The agreement is better for high level AMVs, whatever clustering scheme used. The results are much more scattered for STC versions between each other than for CO2 slicing configurations between each other.

It should be noted that some spectral response characteristics of the Meteosat-8 channels have been changed recently at EUMETSAT, with a clear impact on channel 5 (WV062). Of course these modifications should impact the results of the STC method that use the channel WV062. This study does not take into account these changes, and it is presently difficult to evaluate their consequences on the STC WV062 results. However, it should probably partly explain the difference noted between the WV062 and the WV073.

Figure 5c shows the EBBT pressure versus the CO2 slicing pressure using IR120 channel, for current clustering (left) and new clustering schemes (right). Strange structures appear in the first plot, artificially created by the use of the current clustering process. There is clearly a lack of EBBT pressures around 800 hPa, 600 hPa and 400 hPa. and a lack of CO2 slicing pressures around 200 hPa and 400 hPa. In order to compensate these lacks, an 'accumulation' of EBBT pressures is located at mid level in the troposphere, around 700 hPa, and above 200 hPa for CO2 slicing pressure. These features are the consequences of the mixture of warm and cold radiances into the same cluster, as described above. They do not appear on the second plot of the figure 5c, for which the results look more coherent and consistent. A very good agreement is observed between EBBT and CO2 slicing pressures for high level opaque targets, along the first diagonal under 400 hPa. That is conform to the theoretical expectations and then constitutes a good signal for the consistency of the results as well.

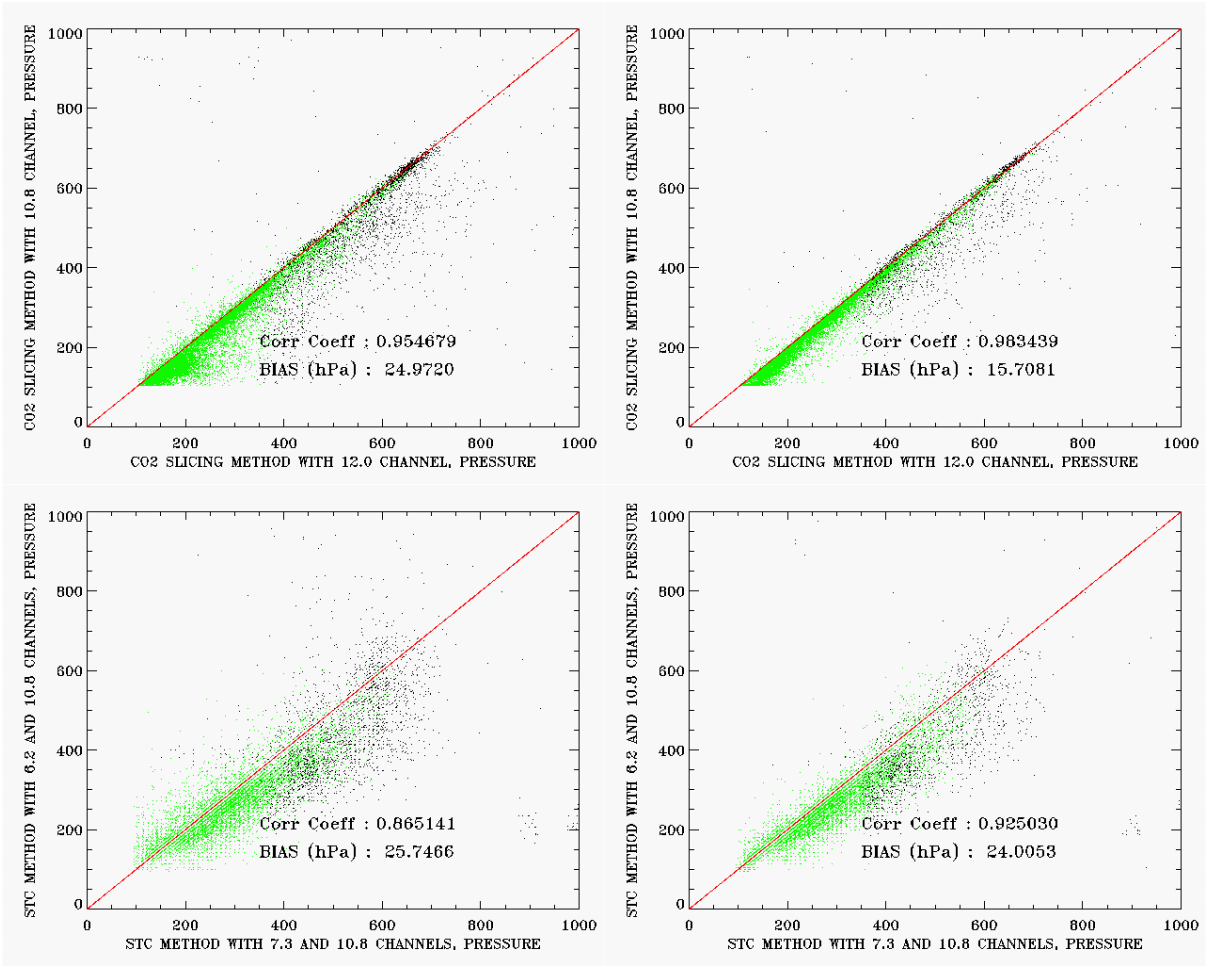

Figure 5b: Consistency of two version of CO2 slicing results (IR108 and IR120) and STC results (WV062 and WV073) between each other. Current clustering scheme comparison is on the left side and the new clustering approach comparison on the right side.

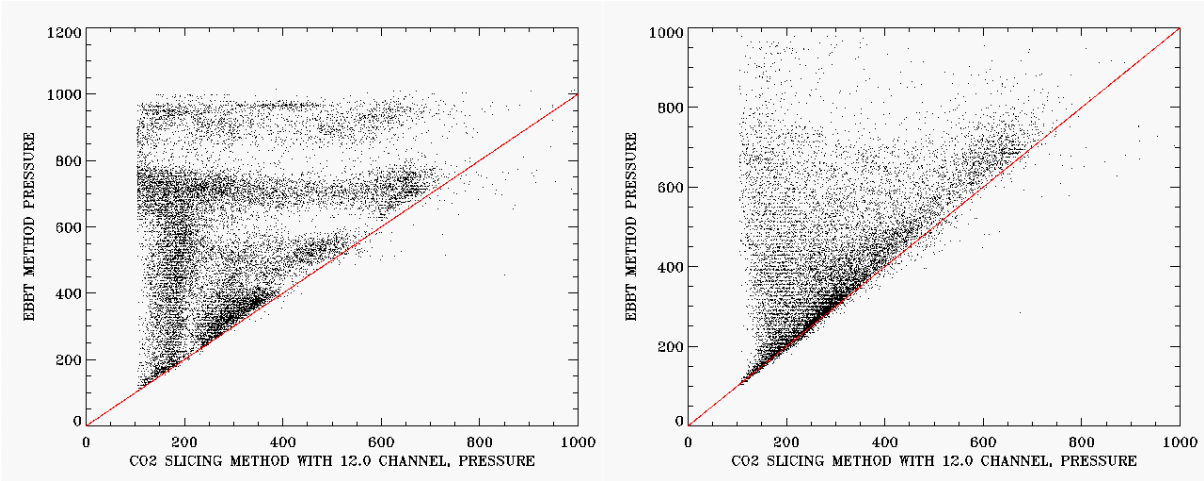

Figure 5c: EBBT pressure versus CO2 slicing pressure (IR120). Current clustering scheme is on the left side and the new clustering approach on the right side.

Sensitivity of the methods to the percentage used.

It has been noted above that pressure calculations may vary a lot with the percentage of coldest cloudy pixels used for the clustering. To understand which percentage is the most adequate to be used for the calculation, its impact on the consistency of HA methods has been examined. Testing the agreement of the methods two by two, the percentage that gives the best consistency can be extracted for this couple of methods. The occurrence for which such percentage gives the best consistency is plotted on figure 6, comparing STC and CO2 slicing configurations. The left plot considers only the couple of pressures that are within a range of 50 hPa together, whereas the right plot considers the couple of pressures within a range of 100 hPa. Consistency of the results given by two different configurations of the same method (CO2120_CO2108, and STC062-STC073) clearly increases when the percentage of cloudy pixels used is decreasing. When the percentage is small, the pixel radiances are more homogeneous and induce nearly the same pressure at the end of the HA process. It can be noted on the plots that CO2 slicing configurations are in a much better agreement between each other than the STC configurations between each other.

The agreement of STC configurations and CO2 120 method does not depend very much on the percentage used.

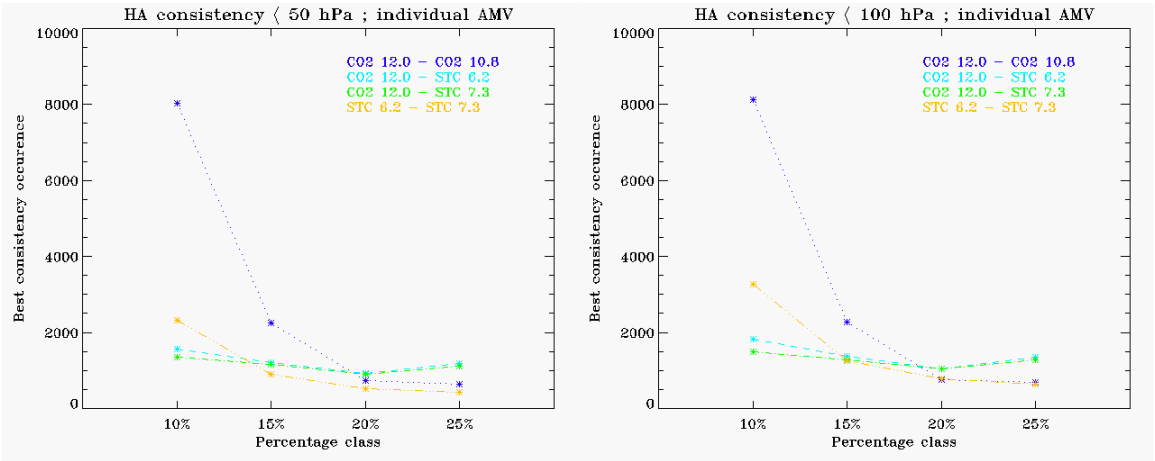

Figure 6: Best consistency of the methods as function of the percentage class.

Impact on the error associated to the pressure

One of the main critical issues of the NWP community is not only to get a good estimation of the AMV height, but also to get an error bar associated to this pressure. All the HA methods implemented at

EUMETSAT calculate an error associated with the pressure. The CO2 slicing method using sample radiances calculate the pressure for all the valid samples within the considered cluster (MSG Algorithm Specification Document EUM.MSG.SPE.022). The final pressure of the cluster and the associated error correspond respectively to the average and the standard deviation of this set of sample pressures. Of course the dispersion of the sample pressures around the mean value depends on the performance of the method, but also on the homogeneity of the input sample radiances. The more homogeneous are the sample radiances the smaller is the error on the pressure.
Figure 7 illustrates histograms of the error associated with the pressure for the set of data described above. The error associated with STC (WV062 and WV073 versions) and CO2 slicing (IR108 and IR120 versions) methods, using current and new clustering (10% percentage) approaches are presented. The new clustering approach tends to select pixels that have the same radiative properties because the clustering criterion is only based on the cloudy radiances. Radiances of valid samples inside a cluster are then closer together and the final error bar associated to the pressure is smaller.
The magnitude of the mean error is divided by a factor 2 for all the methods using the new clustering approach. It is close to 20 hPa for CO2 slicing method. The STC method is generally less accurate with a mean error close to 70 hPa using the 10% new clustering approach, and a significant mean error close to 130 hPa for the STC WV073 configuration using the current clustering. In addition, the shapes of the error histograms are very different. The current clustering artificially creates a strange peak of errors around 70 hPa for the STC configurations. The general distribution of the errors is much more coherent on the second plot for the new approach. Of course the magnitude of the error varies together with the percentage of cloudy pixels used as well. The smaller the percentage the smaller the error bars.

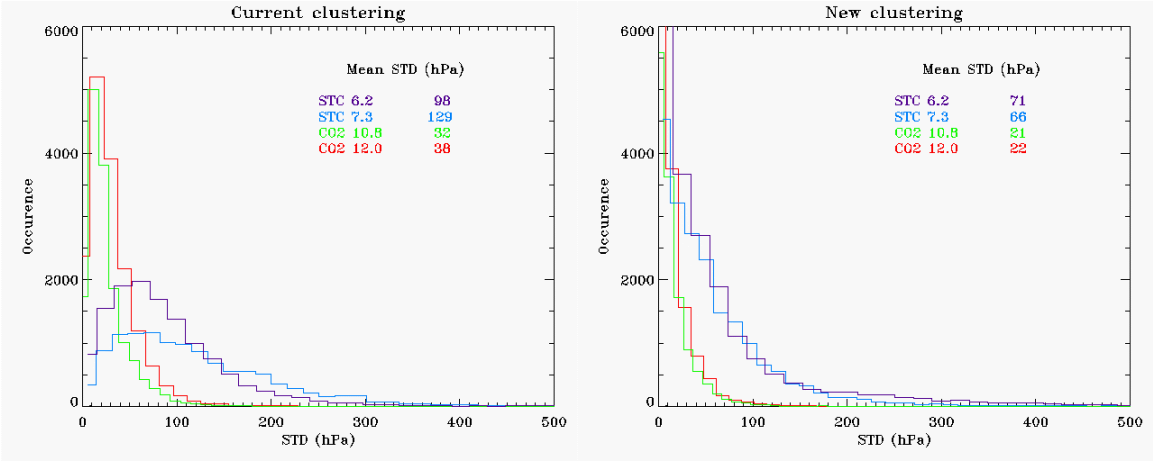

Figure 7: Histograms of the error bar associated to the pressure for STC and CO2 methods, using current and new clustering approaches.

Results against forecast data

This dataset of AMVs extracted from Meteosat 8 images has been compared against forecast winds for the current clustering and the 10% new clustering approaches. Only the AMVs with a speed greater than 2.5 m/s, a Quality Index greater than 0.8, and for which semi transparency correction method has been applied for height calculation, were considered for this test. The 10% cloudy pixels clustering approach improves the results of the correlation coefficient that increases from 0.93 to 0.944 for this dataset, but also reducing the bias from 1.27 m/s to 0.87 m/s. Of course this quick test is not a validation of the method, and a more intensive and longer comparison period against radiosonde observations and NWP analysis is required. Such validation should be done in the framework of the operational environment at EUMETSAT soon.

SUMMARY AND DISCUSSION

The selection of the pixels that are used for the calculation of the height is of crucial importance for the AMV HA process. The current clustering scheme used at EUMETSAT is not always adequate to

calculate the height of AMV, especially when high opaque clouds are located into the target area together with semi-transparent clouds. Unfortunately, this configuration can frequently occur, especially in tropical areas, and the impact on the final pressure set to the AMV is large. The EBBT pressure is especially concerned, due to the blend of cold radiance of high opaque cloud and warm radiance of semi-transparent cloud together into the same cluster.
A new scheme for clustering has been proposed in this paper, mainly based on the brightness radiance of cloudy pixels. The main idea was to select the pixels that really drive the tracking to calculate the height. Several thresholds have been tested, using 10%, 15%, 20% and 25 % of coldest cloudy pixels inside the target area for IR channel.
The results clearly showed the benefits of the new clustering approach on the consistency of the HA methods. Pressures calculated by all the HA methods are in better agreement together using the new scheme. In general the smaller are the percentages of coldest cloudy pixels, the more consistent are the methods between each other. Improvement is also very important on the error associated to the final pressure, which is mainly divided by two using the new approach. For the considered data set, the mean error magnitude is finally around 20 hPa for CO2 slicing methods using the 10% coldest cloudy radiances. For opaque clouds, the EBBT pressure calculated with the new scheme is more coherent, and in better agreement with the theoretical expectations than the current approach. Finally, a quick test on forecast comparison also shows an improvement, decreasing the bias between AMV and forecast speed. Of course a validation over a longer period, against radiosonde observations and forecast analysis is needed to conclude. This validation should be done in the operational framework at EUMETSAT, once the new clustering scheme will be implemented.

Behind this study a more theoretical question is arising concerning the AMVs height assignment. All the methods used for correction of semi-transparency are very sensitive to the input radiances. The EBBT pressure varies also very quickly when the radiances get warmer. That makes an accurate calculation of the final pressure very tricky. Consequently, the main problem consists in selecting the pixels that really drive the tracking step, in order to use only them for the HA calculation. Of course the selection criteria should be directly linked to the tracking scheme itself. The EUMETSAT one is mainly based on the maximum contrast criterion, which ends to favour coldest cloudy pixels in the IR channels. However, the part of the coldest pixels that really contributes to the tracking is difficult to determine, and it certainly does not correspond to a fix percentage of cloudy pixels. Unfortunately, the results of the present paper clearly indicated that the final pressure may vary a lot as function of the percentage used for the HA calculation. A strategy based on adapting percentage values would be more appropriate than a fix threshold. Doing so, it is possible to make a better use of the ‘best possible percentage’ for each AMV as function of its own characteristics. Nevertheless, such selection criteria still remain to be defined and require more investigations. The agreement of the pressures calculated by several HA methods for the same AMV may help in this selection process.

REFERENCES

ASD; ‘MSG Meteorological Products Extraction Facility Algorithm Specification Document’ edited by EUMETSAT. Reference: EUM.MSG.SPE.022

MSG - Cloud Processing, EUMETSAT Technical Memorandum TM-04 written by H.J. Lutz, Dec 1999.

Borde, R., and A. Arriaga, ‘Atmospheric motion vectors height assignment techniques with Meteosat 8’, Proc. Seventh Int. Winds Workshop, Helsinki, Finland, EUMETSAT, EUM P42, pp. 139-145, 2004

De Smet, A.C., ‘Height Assignment with Meteosat 8: our experience so far’, Seventh International Winds Workshop, Helsinki, Finland, EUMETSAT, EUM P42, 147-154, 2004.

Dew, G., and K. Holmlund, Investigations of cross-correlation and Euclidean distance target matching techniques in the MPEF environment, in Proceedings of the Fifth International Winds Workshop, EUMETSAT, EUM P 28, 235– 243, 2000.

Menzel, W.P., W.L. Smith and T. Stewart, Improved cloud motion wind vector and altitude assignment using VAS, *J. Climate Appl. Meteor*., 22, 377-384, 1983

Merill, J. W.P. Menzel, W. Baker, J. Lynch and E. Legg, A report on the recent demonstration of NOAA’s upgraded capability to derive cloud motion satellite winds, *Bull. Amer. Meteor.Soc.*, 72, 372-376, 1991

Nieman, N.J., J. Schmetz and W.P. Menzel, A comparison of several techniques to assign heights to cloud tracers, *, J. Appl. Meteorol.*, 32, 1559-1568, 1993

Schmetz, J., K. Holmlund, J. Hoffman, B. Strauss, B. Mason, V. Gartner, A. Koch, and L. van de Berg, Operational cloud-motion winds from Meteosat infrared images. *J. Appl. Meteor.,* **32,** 1206–1225., 1993

Smith, W.L., and C. M. R. Platt, Intercomparison of radiosonde, ground based laser, and satellite deduced cloud heights. J. Appl. Meter., 18, 1792-1802, 1979.

Schreiner A.J. and P. Menzel, 'Comparison of cloud motion vector height assignment techniques using GOES-12 imager', Sixth International Winds Workshop, Madison Wisconsin, USA (1-10 May 2002), EUMETSAT, EUM P35, 301-305, 2002.

Schreiner A.J., P. Menzel, A. Heidinger, J. Davis and W. Feltz, 'Comparison of cloud motion vector height assignment techniques using the GOES-12 imager', Seventh International Winds Workshop, Helsinki, Finland, EUMETSAT, EUM P42, 163-170, 2002.